



HAL
open science

Chemical effects of ferrocene and 2-ethylhexyl nitrate on a low-octane gasoline: An experimental and numerical RCM study

Minh Duy Le, Mickaël Matrat, Arij Ben Amara, Fabrice Foucher, Bruno Moreau, Yi Yu, Pierre-Alexandre Glaude

► To cite this version:

Minh Duy Le, Mickaël Matrat, Arij Ben Amara, Fabrice Foucher, Bruno Moreau, et al.. Chemical effects of ferrocene and 2-ethylhexyl nitrate on a low-octane gasoline: An experimental and numerical RCM study. Proceedings of the Combustion Institute, 2021, 38 (1), pp.441-448. 10.1016/j.proci.2020.06.191 . hal-03226556

HAL Id: hal-03226556

<https://hal.science/hal-03226556>

Submitted on 24 Apr 2023

HAL is a multi-disciplinary open access archive for the deposit and dissemination of scientific research documents, whether they are published or not. The documents may come from teaching and research institutions in France or abroad, or from public or private research centers.

L'archive ouverte pluridisciplinaire **HAL**, est destinée au dépôt et à la diffusion de documents scientifiques de niveau recherche, publiés ou non, émanant des établissements d'enseignement et de recherche français ou étrangers, des laboratoires publics ou privés.



Distributed under a Creative Commons Attribution - NonCommercial 4.0 International License

Chemical Effects of Ferrocene and 2-Ethylhexyl Nitrate on a Low-Octane Gasoline: an Experimental and Numerical RCM Study

Minh Duy Le^{a,c}, Mickaël Matrat^{a,*}, Arij Ben Amara^a, Fabrice Foucher^b, Bruno Moreau^b, Yi Yu^b,
Pierre-Alexandre Glaude^c

^a*IFP Energies Nouvelles, 1 et 4, avenue de Bois-Préau, 92852 Reuil-Malmaison Cedex, France*

^b*Univ. Orléans, INSA-CVL, PRISME, EA 4229, F45072, Orléans, France*

^c*LRGP, CNRS-Université de Lorraine, 1, rue Grandville, 54000 Nancy, France*

Colloquia: GAS-PHASE REACTION KINETICS

Total length of paper: 5996 words

List of word equivalent lengths for main text, references, each figure and each table

Item	Word equivalent lengths
Main text	3624
Equation (1)	23
References	717
Figure 1	338
Figure 2	189
Figure 3	337
Figure 4	194
Figure 5	287
Figure 6	289

All supplementary materials are submitted with this paper.

* Corresponding author: mickael.matrat@ifpen.fr; Tel: +33 1 47 5251 10

List of figure captions

Figure	Caption
Figure 1	IDT of the neat surrogate fuel (black) and the surrogate fuel doped with 0.1% mol. ferrocene (grey) at 10 bar. Experiments: filled symbols (main IDT) and empty symbols (1 st -stage IDT). Simulation: solid lines (main IDT) and dashed lines (1 st -stage IDT). (a) $\Phi = 1$, (b) $\Phi = 0.5$. Simulations with the initial kinetic model.
Figure 2	Simulated profiles of iron species during a RCM test at condition: 10 bar, 830 K, $\Phi = 1$, surrogate fuel doped with 0.1% mol. ferrocene. Simulation with the initial kinetic model.
Figure 3	IDT of the neat surrogate fuel (black) and the surrogate fuel doped with 0.1% mol. ferrocene (grey) at 10 bar. Experiments: filled symbols (main IDT) and empty symbols (1 st -stage IDT). Simulations by the new kinetic model: solid lines (main IDT) and dashed lines (1 st -stage IDT). (a) $\Phi = 1$, (b) $\Phi = 0.5$.
Figure 4	Measured (solid line) and simulated (dashed line) of pressure histories near the top dead center during RCM experiments at $P_c \approx 10$ bar, $\Phi = 1$, $T_c = 915$ K of the neat surrogate fuel (black lines), the surrogate fuel doped with EHN 0.1% mol (thick grey lines) and the surrogate fuel doped with ferrocene 0.1% mol. (thin grey lines).
Figure 5	Reactions pathway of toluene at 10 bar, $\Phi = 0.5-1$, 675 K-1000 K and the reactions representing effects of EHN and ferrocene on toluene reactivity.
Figure 6	Reactions pathway of <i>n</i> -heptane at 10 bar, $\Phi = 1$, 830 K and the reactions representing effects of EHN and ferrocene on NTC behavior.

Abstract

An in-depth understanding of fuel additives chemical effects is crucial for optimal use or additive design dedicated to more efficient and cleaner combustion. This study aims at investigating the effect of an organometallic octane booster additive named ferrocene on the combustion of a low-octane gasoline at engine-relevant conditions. Rapid compression machine experiments were carried out at 10 bar, from 675 to near 1000 K for stoichiometric ($\Phi = 1$) and lean ($\Phi = 0.5$) mixtures. The neat surrogate fuel was a blend of toluene and *n*-heptane whose research octane number was 84. The doping level of additive was set at 0.1% molar basis. Ferrocene does not show a remarkable effect on the 1st-stage ignition but presents a strong inhibiting effect on the main ignition of the surrogate fuel at both equivalence ratios. The inhibiting effect increases with temperature within the investigated range. The negative temperature coefficient (NTC) behavior of the surrogate fuel is enhanced by ferrocene. A kinetic model developed by literature data assembly as well as a novel sub-mechanism involving the formation of alcohols from the reactions of iron species is proposed. The kinetic model developed simulates the inhibiting effect of ferrocene reasonably well at both equivalence ratios. Thanks to the validated kinetic model, the chemical effect of ferrocene on the fuel combustion is explored and compared with 2-ethylhexyl nitrate (EHN), which is a conventional reactivity enhancer. Three major differences between the two additives were identified: the high-temperature stability of the fuel additive, the influence of additive on the toluene reactivity and the effect of the additive on the NTC behavior. The results presented in this study contribute to the in-depth comprehension of chemical effect of two fuel additives (ferrocene and EHN) having opposite effects on fuel reactivity.

Key words

Fuel additive; ferrocene; 2-ethylhexyl nitrate; rapid compression machine; EHN; kinetic modeling; low temperature combustion.

1. Introduction

Internal combustion (IC) engine development currently focuses on more efficient and cleaner combustion to reduce exhaust gas emissions. Low temperature combustion (LTC) [1] is getting a lot of attention from engine researchers thanks to its low-emission operation. Moreover, this combustion strategy can be employed in many engines such as homogeneous charge compression ignition (HCCI) engine [2], gasoline compression ignition (GCI) engine [3], etc..

To improve the combustion quality in engines, fuel additives have been studied and commercialized for decades. Conventional fuel combustion additives can be divided into two categories as octane boosters and cetane boosters. These two types of additives have an opposite effect on fuel reactivity. Octane boosters are employed to lower fuel reactivity to avoid knock in spark-ignition (SI) engines. Typical octane boosters include organometallics [4,5], aromatic amines [6], and oxygenated compounds [7,8]. On the other hand, cetane boosters based on nitrates and peroxides compounds [9,10] are used to increase the reactivity of diesel fuels.

Despite the wide use of fuel additives, the understanding of their chemical effect on the fuel combustion is still limited. A deeper understanding of a fuel additive is essential not only for the optimal use of this additive but also for the design of a new additive which is capable of making combustion more efficient and cleaner. 2-Ethylhexyl nitrate (EHN) and ferrocene are two of the most fundamentally studied additives in literature. EHN is a conventional cetane booster. This additive has been investigated in various fuels under different engine-relevant conditions [11–14]. A recent study

on EHN from our group [14] is dedicated on understanding its chemical effect which mostly relies on the chemistry of nitrogen oxides (NO and NO₂). Ferrocene is a high efficient octane booster. This molecule has an atom of iron stored between two cyclopentadienyl groups. Though the use of ferrocene decreases because of the formation of iron deposits on the spark plug, this additive was being employed in several countries within an acceptable doping level in the early 2000 [15]. The studies on ferrocene are still scarce. Most experimental researches on this additive in literature were obtained with flame studies [16–21]. Recently, Fenard et al. [22] conducted experiments in a rapid compression machine (RCM) at relatively low temperatures (< 850 K) to investigate the effect of ferrocene on the combustion of iso-octane and 3-hexene. This study suggests that the chemical effect might be related to the reactions of HO₂ and H₂O₂ on the surface of iron oxide particles. The inhibiting effect of ferrocene was underestimated by the kinetic model assembled in this study. The difference between experimental and simulation results shown in the study of Fenard et al. [22] suggests that further investigations on ferrocene are necessary to explain the inhibiting effect of this additive. Quantum chemical calculations are powerful and provide a significant insight into key reaction properties including rate constant, products speciation and thermochemical data [23,24]. However, it is challenging to employ this method to study iron chemistry as the element is a first-row transition metal. Iron is remarkably heavier than an atom of carbon, hydrogen, oxygen or nitrogen. Iron species, as well as other transition metal compounds, can present a multi-reference behaviour. This implies that the non-dynamical correlation must be included in quantum calculations to get reliable results. This feature

makes the calculations computationally too expensive [25].

To fulfill the lack of fuel additive study in literature, this study aims at (1) investigating experimentally and numerically the inhibiting effect of ferrocene at LTC relevant conditions, and (2) presenting the most notable differences between the chemical effects of a cetane booster (EHN) and an octane booster (ferrocene). The ignition delay time (IDT) measurements were conducted in a RCM. Modeling work was carried out to simulate the effect of ferrocene.

2. Experimental Methods

Experimental IDT measurements were conducted at the single-piston RCM of the University of Orleans. This RCM consists of a creviced piston to avoid the vortex formation and maintains the post-combustion charge homogeneity. The use of a creviced piston helps to study the hydrocarbon autoignition chemistry limiting physical effects. The piston is pneumatically driven and braked close to the top dead center by hydraulic technique. The total duration of compression is about 33 ms. The pressure at the top dead center is noted as P_c . The pressure rises from $P_c/2$ to P_c within 3.5 ms (t_{50}). The position of the piston was measured with a linear displacement sensor. The lengths of the stroke and the bore of the RCM are 300 mm and 50 mm respectively. The compression ratio is adjusted from 8.9 to 20.7 to get the desired experimental conditions. The measurement uncertainties of in-cylinder pressure, intake pressure, intake temperatures, and mass flow rate are $\pm 1\%$, ± 1 mbar, ± 2 K and $\pm 1\%$, respectively. Further details of the RCM of the University of Orleans can be accessed elsewhere [13,26].

In this work, the high purity chemical compounds including toluene (99.8%), *n*-heptane (99%), ferrocene (97%) from Sigma-Aldrich were employed. The surrogate fuel is a mixture of toluene (65% vol.) and *n*-heptane (35% vol.). The IDT of this surrogate was experimentally measured at 10 bar, from 675 K to near 950 K at Φ of 0.5 and 1 in previous studies [13,14]. This surrogate fuel is designed to observe the additive effect on specific combustion properties such as two-stage ignition and negative temperature coefficient (NTC). Ferrocene doping level was set at 0.1% mol. with a relative uncertainty below 1%. The doped fuels were gravimetrically prepared. To obtain the desired equivalence ratio, the gaseous fuel was premixed with the synthetic air (21% O₂, 79% N₂) from Air Liquide in a reservoir. The composition of gas mixtures investigated in this study is presented in table S1. The uncertainty in molar fraction is about 5%. The temperature of the reservoir was maintained at 80°C. The homogeneity of each gas mixture was ensured by a mechanic agitation during 30 minutes. All gas mixtures were prepared on the day of the experiment.

For each RCM test, the pressure at top dead center ($P_c = 10$ bar) and the temperatures at top dead center (T_c) were obtained by adjusting the intake pressure ($227 \text{ mbar} < P_0 < 600 \text{ mbar}$) and the piston initial temperature ($55 \text{ }^\circ\text{C} < T_0 < 120 \text{ }^\circ\text{C}$). The vapor pressure of ferrocene calculated with the formula reported by Jacobs et al. [27] is compared to the partial pressure of this additive contained in the fuel reservoir and in the combustion chamber initial conditions to conclude that there was no condensation of ferrocene during experimental tests. The T_c are calculated by applying isentropic relation as presented in equation (1), where γ is the ratio of specific heats of gas mixture:

$$\int_{T_0}^{T_c} \frac{\gamma}{\gamma - 1} \frac{dT}{T} = \ln \left(\frac{P_c}{P_0} \right) \quad (1)$$

In this study, the main IDT is defined as the duration between the end of compression and the combustion Maximum Pressure Rise Rate (MPRR). The last value corresponds to the peak of dP/dt profile. In the case of two-stage ignitions, the 1st-stage IDT is measured as the time between the end of compression and the first distinguishable peak of dP/dt . The standard deviation of 1st-stage IDT and main IDT in this work are $\pm 10\%$ and $\pm 5\%$ respectively.

3. Kinetic modeling

To investigate the ferrocene additive effect on the surrogate fuel reactivity, a detailed kinetic model was developed in this work. The surrogate fuel sub-mechanism, based on the kinetic model of Lawrence Livermore National Laboratory (LLNL) [28], was fully adopted from a previous work [13]. The validation of this sub-mechanism was obtained with a large set of experimental data from literature and for several toluene/ *n*-heptane mixtures [13,14,29,30].

The ferrocene sub-mechanism was built based on literature. It consists of three groups of reactions including ferrocene decomposition, interactions of small radicals (H, O, OH, HO₂) with ferrocene and reactions of iron species. The first two groups of reactions were adopted from the work of Fenard et al. [22]. The ferrocene decomposition was described as a two-step decomposition. Firstly, ferrocene (FeC₁₀H₁₀) released a cyclopentadienyl radical (C₅H₅) to produce FeC₅H₅. The rate constant of this reaction was adopted from the work of Lewis et al. [31]. The second step was a dissociation to produce Fe and C₅H₅. The kinetic of this reaction was estimated by Hirasawa et al. [17]. The rate of the reactions

of small radicals with ferrocene was estimated by Fenard et al. [22] based on literature data [17,32,33]. Table S2 summarizes all the reactions involving ferrocene and FeC_5H_5 in the current study. Iron species reactions including iron (Fe), iron oxides (FeO , FeO_2), iron hydroxides (FeOH , $\text{Fe}(\text{OH})_2$) and other iron compounds (FeOOH , FeH) were adopted from the study of Rumminger et al. [34]. Additionally, the kinetic model includes the reaction of Fe with NO_2 [35] and CO_2 [36]. The reactions of nucleation of Fe atoms from the work of Wen et al. [37] were added in the kinetic model.

In this study, the measured IDT were simulated thanks to the 0-D closed homogenous reactor model in CHEMKIN-PRO [38]. The chemical reactivity of the gas mixture during the compression process was considered. The initial thermodynamic condition of a simulation were the intake pressure (P_0) and the piston initial temperature (T_0). The heat loss during a RCM experiment was taken into account by using an “effective volume”. This “effective volume” profile was obtained by conducting a non-reactive experiment where O_2 was replaced by N_2 at the same initial conditions as those of the targeted reactive experiments. The calculation of the adiabatic core hypothesis was then applied to deduce the volume profile as described by Tanaka et al. [39].

4. Results and Discussions

This section investigates experimentally and numerically the IDT of ferrocene doped fuel. The objective is to better assess its chemical activity in order to explore the chemistry of two opposite additives, i.e. ferrocene and EHN.

4.1. Effect of ferrocene on the reactivity of the fuel surrogate

The ferrocene effect on the fuel surrogate reactivity is presented in Figure 1 for two equivalence ratios at 10 bar from near 675 K to near 1000 K. The doping level of ferrocene was set at 0.1% mol.. The reactivity of the neat surrogate fuel depends on the equivalence ratio. A strong NTC behavior is observed from 790 K to around 885 K at $\Phi = 1$. Two-stage ignitions exist at the lower temperature range ($T_c < 790$ K) for both equivalence ratios. While ferrocene does not show a remarkable effect on the 1st-stage ignition of the surrogate fuel, this additive presents a strong inhibiting effect on the main ignition. The latter effect increases with temperature. The main IDT of the doped fuel is up to 4 times longer than one of the neat fuel at the highest examined temperatures ($T_c > 900$ K). In addition, ferrocene enhances the NTC behavior of the surrogate fuel. In lean conditions ($\Phi = 0.5$), the doped fuel presents an NTC behavior from 750 K to 910 K which is not observed in the case of the neat fuel.

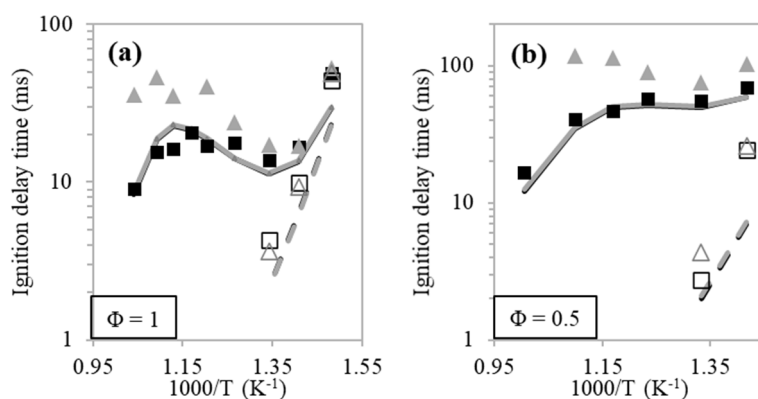


Figure 1. IDT of the neat surrogate fuel (black) and the surrogate fuel doped with 0.1% mol. ferrocene (grey) at 10 bar. Experiments: filled symbols (main IDT) and empty symbols (1st-stage IDT). Simulation: solid lines (main IDT) and dashed lines (1st-stage IDT). (a) $\Phi = 1$, (b) $\Phi = 0.5$. Simulations with the initial kinetic model.

The initial kinetic model based on available data strongly underestimates the ferrocene effect as presented in Figure 1. Simulations with or without the addition of ferrocene lead to similar ignition delay times. This kinetic model is limited to ferrocene and iron chemistry from Fenard et al. [22] and

Rumminger et al. [34]. Ferrocene decomposition was experimentally investigated [31]. As a first approximation, the interactions of ferrocene with key combustion radicals (O, H, OH, HO₂) were estimated based on similar reactions of alkenes with these radicals [22]. The reactions of other iron species were included from the model of Rumminger et al. [34] to simulate the very high temperature ($T > 2000$ K) reactivity [34], which is not relevant to the experimental condition examined in this study. All above estimations are limited to describe the ferrocene effect under the conditions investigated in this work.

4.2. Ferrocene sub-mechanism improvement

The inability of the initial model to replicate the experimental observations indicated that some reaction pathways may be missing in the ferrocene sub-mechanism. It was hypothesized that some reactions between iron species and radicals derived from parent fuels might play a role and should be included in the kinetic model. In order to quantify the relative amounts of the different iron-containing species, Figure 2 presents the simulated profiles of iron species in conditions, in which ferrocene was experimentally found to be effective (see Figure 1), i.e. 10 bar, 830 K, $\Phi = 1$, doping level of ferrocene at 0.1% mol. The simulation is conducted with the initial kinetic model.

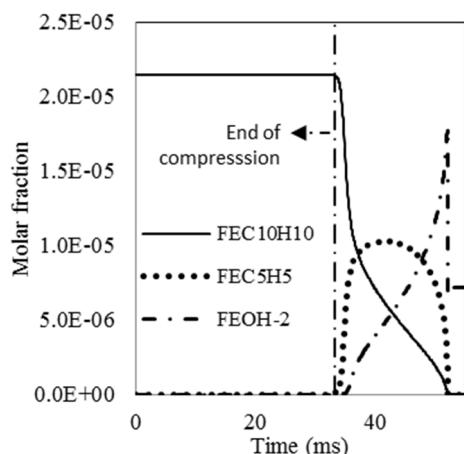


Figure 2. Simulated profiles of iron species during a RCM test at condition: 10 bar, 830 K, $\Phi = 1$, surrogate fuel doped with 0.1% mol. ferrocene. Simulation with the initial kinetic model.

The most dominant simulated iron species are $\text{FeC}_{10}\text{H}_{10}$, FeC_5H_5 and $\text{Fe}(\text{OH})_2$. Their chemistries were assumed to be the most important involved in the inhibiting effect of ferrocene. Rate constants of reactions involving ferrocene with atoms and small radicals (H, O, OH, HO_2) presented in table S2 in the Supplementary Document were thus reviewed. Performing a brute sensitivity analysis on these rate constants, it was found that only reactions of $\text{FeC}_{10}\text{H}_{10}$ and FeC_5H_5 with HO_2 provided an inhibiting effect at $T_c < 885$ K. Similar reactions were then applied to represent the interactions of $\text{FeC}_{10}\text{H}_{10}$ and FeC_5H_5 and other dominant peroxy radicals (CH_3OO , $\text{C}_2\text{H}_5\text{OO}$, and $\text{C}_6\text{H}_5\text{CH}_2\text{OO}$). All these reactions produced the corresponding alcohols (CH_3OH , $\text{C}_2\text{H}_5\text{OH}$, and $\text{C}_6\text{H}_5\text{CH}_2\text{OH}$). At this step, the new model could simulate the effect of ferrocene at $T_c < 885$ K but not at $T_c > 885$ K. To extend the model performance, the chemistry of $\text{Fe}(\text{OH})_2$ was updated because of its significant concentration in the high temperature range. Thanks to the above proposed reactions with $\text{FeC}_{10}\text{H}_{10}$ and FeC_5H_5 , the inhibiting effect of ferrocene is supposed to be related to the radical-consuming reactions producing low reactive species. Novel reactions between the radicals (OH, CH_3 , C_2H_5 , and

$C_6H_5CH_2$) with $Fe(OH)_2$ forming the corresponding alcohols were thus included in the mechanism. These reactions were numerically identified as the main source of the ferrocene inhibiting effect at $T_c > 885$ K. Table S3 in the Supplementary Document summarizes the new proposed reactions involving $FeC_{10}H_{10}$, FeC_5H_5 and $Fe(OH)_2$. The activation energy and pre-exponential factor estimations were based on the work of Rumminger et al. [34] in which the reference reactions of iron species were mostly barrierless. The proposed sub-mechanism captures the fuel additive effect suggesting that such inhibiting behavior could be a viable pathway to explain the ferrocene activity in the tested operating conditions.

Figure 3 illustrates the new simulation results in comparison with the experimental data. At the stoichiometric condition, the inhibiting effect of ferrocene on the main IDT of the surrogate fuel over the whole range of examined temperatures is correctly captured. The model predicts an inhibiting effect on the 1st-stage IDT while this cannot be confirmed clearly experimentally. Overall, the proposed kinetic mechanism simulates reasonably the experimental measurements at two equivalences ratio investigated in this study. The resulting chemical mechanism developed and used in this study is provided in Supplementary Materials of this paper.

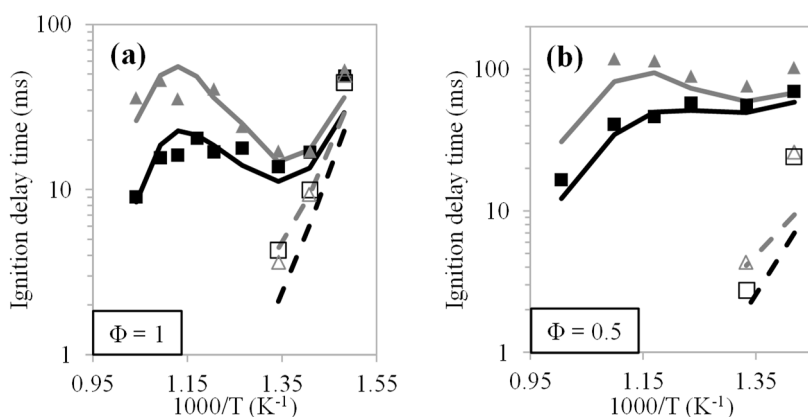


Figure 3. IDT of the neat surrogate fuel (black) and the surrogate fuel doped with 0.1% mol. ferrocene (grey) at 10 bar. Experiments: filled symbols (main IDT) and empty symbols (1st-stage IDT). Simulations by the new kinetic model: solid lines (main IDT) and dashed lines (1st-stage IDT). (a) $\Phi = 1$, (b) $\Phi = 0.5$.

4.3. Differences between chemical effects of ferrocene (an octane booster) and EHN (a cetane booster)

While the use of additives to modify hydrocarbons reactivity has been investigated thoroughly in the past, discussions on the additives chemical effects are not frequent. The kinetic model developed in this study has the advantage to be developed for both iron involving species and nitrogen containing ones. More specifically, both the chemistries of an octane booster (ferrocene) and of a cetane booster (EHN) are included and validated upon a large set of existing experimental data. The latter was experimentally and numerically investigated in a previous study using the same RCM of Orléans [13,14]. A comparison of the two additives is carried out to highlight the differences of chemical activities, which could be of interest for further additives development. The simulations of fuel doped with EHN presented in the next figures were carried out with the kinetic model developed in the previous study [14]. Rate of production (ROP) analyses were conducted at the time corresponding to 80% EHN decomposition.

The first difference between the two additives is related to their decompositions during RCM tests.

Simulations were performed at $P_c = 10$ bar, $T_c = 915$ K, $\Phi = 1$ and the doping levels of EHN and ferrocene were set at 0.1% mol. in the surrogate fuel. By simulations, it was observed that EHN decomposed before the end of compression while ferrocene remained stable. The early decay of EHN initiated the combustion of toluene and *n*-heptane and then increased P_c . Figure 4 presents the pressure histories near the end of compression of RCM tests with the neat and doped fuels. In the presence of EHN, P_c increased remarkably. The pressure histories of the neat and doped fuels were reasonably simulated. This also highlighted the correct behavior of the kinetic model of this study.

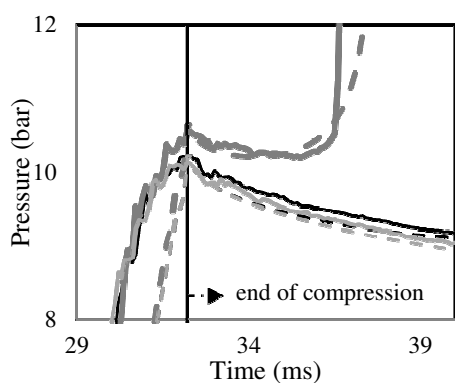


Figure 4. Measured (solid line) and simulated (dashed line) of pressure histories near the top dead center during RCM experiments at $P_c \approx 10$ bar, $\Phi = 1$, $T_c = 915$ K of the neat surrogate fuel (black lines), the surrogate fuel doped with EHN 0.1% mol (thick grey lines) and the surrogate fuel doped with ferrocene 0.1% mol. (thin grey lines).

The second difference between the two additives is related to their interactions with toluene. Figure 5 illustrates how toluene reacts under the investigated conditions (10 bar, $\Phi = 0.5 - 1$, 675 K - 1000 K). Toluene forms primarily benzyl radical ($C_6H_5CH_2$) by H-atom abstraction. This radical undergoes an O_2 addition to form benzyl peroxy radical ($C_6H_5CH_2OO$). This compound is much less reactive than heptyl peroxy isomer radicals because of the lack of a facile intramolecular isomerization reaction, and reacts mostly in termination steps. The previous study [14] showed that this additive

forms NO_2 , which can react with benzyl radical ($\text{C}_6\text{H}_5\text{CH}_2$) to produce NO and $\text{C}_6\text{H}_5\text{CH}_2\text{O}$. This last radical is more reactive than $\text{C}_6\text{H}_5\text{CH}_2\text{OO}$ as it quickly decomposes into H-atom and benzaldehyde ($\text{C}_6\text{H}_5\text{CHO}$). In the presence of ferrocene, this additive decelerates the toluene reactivity by a set of different reactions (R2, R3, and R4): ferrocene and its derived compounds (FeC_5H_5 , $\text{Fe}(\text{OH})_2$) react with $\text{C}_6\text{H}_5\text{CH}_2$ and $\text{C}_6\text{H}_5\text{CH}_2\text{OO}$ radicals to produce the low reactivity alcohol $\text{C}_6\text{H}_5\text{CH}_2\text{OH}$.

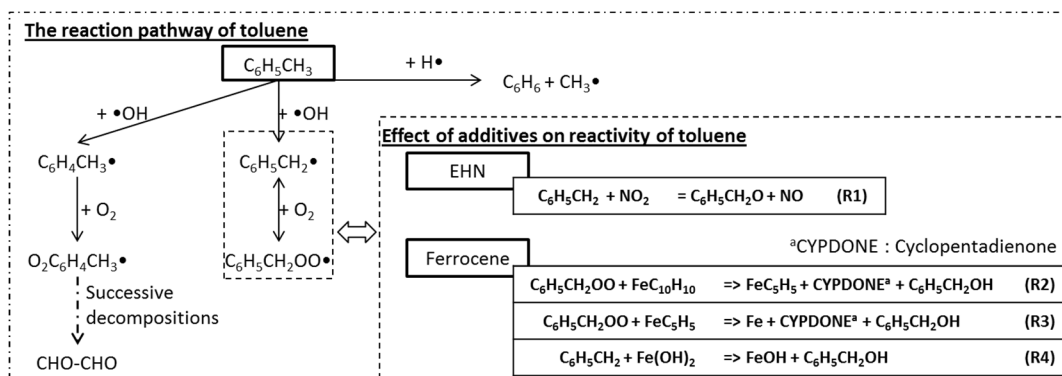


Figure 5. Reactions pathway of toluene at 10 bar, $\Phi = 0.5-1$, 675 K-1000 K and the chemical effects of EHN and ferrocene on toluene reactivity.

The last difference between the two additives is their effect on the NTC behavior. It was found that EHN could mitigate the NTC behavior of the surrogate fuel [14]. In this study, the experiment results indicate that ferrocene enhances this phenomenon. The NTC behavior of the surrogate fuel comes from the chemistry of *n*-heptane. Figure 6 presents the reaction pathway of *n*-heptane at $P_c = 10$ bar, $T_c = 830$ K, $\Phi = 1$ for three fuels: the neat surrogate fuel, the surrogate fuels doped with EHN 0.1 % mol. and with ferrocene 0.1% mol.. The main reason for the NTC phenomenon involves the reactions of heptyl peroxy radicals ($\text{C}_7\text{H}_{15}\text{OO}$) and their isomer hydroperoxy heptyl radicals ($\text{C}_7\text{H}_{14}\text{OOH}$). At intermediate temperature ($T_c = 830$ K), the formations of alkenes and cyclic ethers from $\text{C}_7\text{H}_{15}\text{OO}$ and $\text{C}_7\text{H}_{14}\text{OOH}$ are favored compared to the second oxygen addition leading to the

formation of ketohydroperoxides, which results in branching agents. These reactions slow down the reactivity of *n*-heptane and the surrogate fuel. The NO₂ formation from EHN also leads to the benzyl radical oxidation (C₆H₅CH₂) and produces NO and C₆H₅CH₂O. NO then reacts with C₇H₁₅OO through reaction R5 which enhances the reactivity and restrains the NTC zone. Conversely, ferrocene enables the reactions R6 and R7 with HO₂. The consumption of HO₂ radicals released from C₇H₁₅OO decomposition accelerates this latter reaction forming alkenes. Consequently, the NTC phenomenon is expanded.

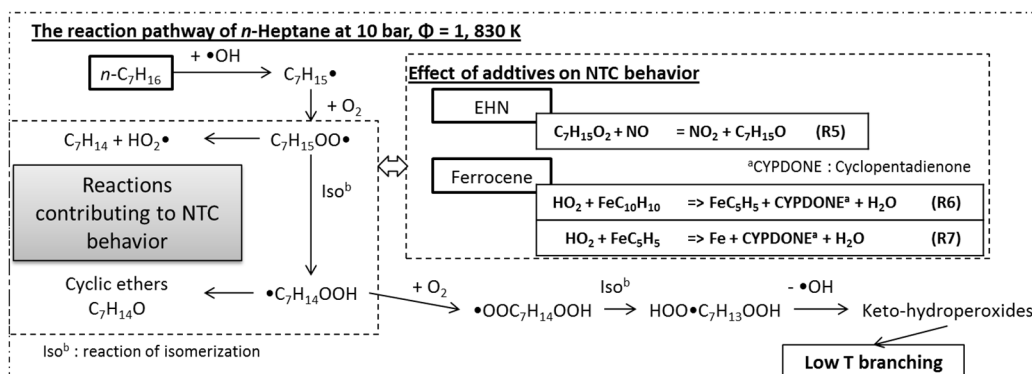


Figure 6. Reactions pathway of *n*-heptane at 10 bar, $\Phi = 1$, 830 K and the chemical effects of EHN and ferrocene on NTC behavior.

In conclusion, three main differences on two opposite additives regarding their effect on a surrogate fuel reactivity are described. They involve their stability, their impact on toluene reactivity and on the NTC behavior mostly related to *n*-heptane.

5. Conclusions

This study investigates experimentally and numerically the inhibiting effect of ferrocene under engine-relevant conditions. To measure IDT, experiments were conducted in a RCM at $\Phi = 0.5$ and 1, $P_c = 10$ bar and $T_c = 675 - 1000$ K. The neat surrogate fuel is a mixture of toluene and *n*-heptane to

evaluate the additive effect on key combustion properties such as two-stage ignition or NTC. The doping level of ferrocene was set at 0.1% mol.

It was found that ferrocene did not show a remarkable effect on the 1st-stage ignition of the surrogate fuel. However, ferrocene showed a strong inhibiting effect on the main ignition of the surrogate fuel at both equivalence ratios. This effect increases with T_c . Ferrocene enhances surrogate fuel NTC.

A kinetic model was developed with literature data assembly. This model failed to reproduce the effect of ferrocene emphasizing the need for a novel mechanism. Additional reactions involving the formation of low reactivity species from the reactions of iron species with radicals such as HO_2 , $C_6H_5CH_2$, $C_6H_5CH_2OO$ were proposed. The new model successfully simulated the inhibiting effect of ferrocene at both equivalence ratios.

Thanks to the validated kinetic model of ferrocene, the chemical effect of this additive on the fuel combustion is described. Compared with EHN, which is a conventional reactivity enhancer, three differences are demonstrated. The first difference is about the stability of the fuel additive as Ferrocene is much more stable than EHN. The second is related to the additive chemical effect on the fuel surrogate. While EHN promotes the toluene oxidation with the interaction of NO_2 and benzyl radical, ferrocene slows down the toluene oxidation thanks to reactions producing an alcohol. The reactions of benzyl and benzyl peroxy radicals with iron species enables this pathway. This mechanism could also describe the chemical effect of these additives with other aromatic fuels such as (poly) methylbenzene.

The last difference reveals how these two additives affect the NTC behavior. EHN mitigates the NTC zone through the reaction of heptyl peroxy isomer radicals with NO while ferrocene raises NTC phenomenon by consuming the HO₂ radical released from heptyl peroxy isomer radicals.

This study contributes to the fundamental understanding of additives impact in different temperature or composition conditions. Original experimental data were used to propose a novel chemical mechanism capable of simulating and exploring inhibiting and enhancing additive effects. Future studies will be dedicated to fuel surrogates involving oxygenated hydrocarbons to characterize the additives effect on an extended set of hydrocarbons.

References

- [1] A.K. Agarwal, A.P. Singh, R.K. Maurya, Evolution, challenges and path forward for low temperature combustion engines, *Progress in Energy and Combustion Science* 61 (2017) 1–56.
- [2] F. Zhao, Homogeneous charge compression ignition (HCCI) engines: Key research and development issues, Society of Automotive Engineers, Warrendale PA, 2003.
- [3] G. Kalghatgi, B. Johansson, Gasoline compression ignition approach to efficient, clean and affordable future engines, *Proceedings of the Institution of Mechanical Engineers, Part D: Journal of Automobile Engineering* 232 (2017) 118–138.
- [4] D. Seyferth, The Rise and Fall of Tetraethyllead. 2, *Organometallics* 22 (2003) 5154–5178.
- [5] V.E. Emel'yanov, L.S. Simonenko, V.N. Skvortsov, Ferrocene - A nontoxic antiknock agent for automotive gasolines, *Chemistry and Technology of Fuels and Oils* 37 (2001) 224–228.
- [6] C.F. Cullis, J.M. Holwill, R.T. Pollard, The influence of amines on the combustion of n-heptane, *Symposium (International) on Combustion* 13 (1971) 195–203.
- [7] V.S.B. Shankar, M. Al-Abbad, M. El-Rachidi, S.Y. Mohamed, E. Singh, Z. Wang, A. Farooq, S.M. Sarathy, Antiknock quality and ignition kinetics of 2-phenylethanol, a novel lignocellulosic octane booster, *Proc. Combust. Inst.* 36 (2017) 3515–3522.
- [8] A. da Silva Jr., J. Hauber, L.R. Cancino, K. Huber, The research octane numbers of ethanol-containing gasoline surrogates, *Fuel* 243 (2019) 306–313.
- [9] W.E. Robbins, R.R. Audette, N.E. Reynolds, Performance and Stability of Some Diesel Fuel Ignition Quality Improvers, SAE Technical Paper 510200 (1951).
- [10] A.B. Rode, K. Chung, Y.-W. Kim, I.S. Hong, Synthesis and Cetane-Improving Performance of 1,2,4,5-Tetraoxane and 1,2,4,5,7,8-Hexaoxonane Derivatives, *Energy Fuels* 24 (2010) 1636–1639.
- [11] M. Hartmann, K. Tian, C. Hofrath, M. Fikri, A. Schubert, R. Schießl, R. Starke, B. Atakan, C. Schulz, U. Maas, F. Kleine Jäger, K. Kühling, Experiments and modeling of ignition delay times, flame structure and intermediate species of EHN-doped stoichiometric n-heptane/air combustion, *Proc. Combust. Inst.* 32 (2009) 197–204.
- [12] S.S. Goldsborough, M.V. Johnson, C. Banyon, W.J. Pitz, M.J. McNenly, Experimental and modeling study of fuel interactions with an alkyl nitrate cetane enhancer, 2-ethyl-hexyl nitrate, *Proc. Combust. Inst.* 35 (2015) 571–579.
- [13] M. D. Le, M. Matrat, A. Ben Amara, F. Foucher, B. Moreau, Y. Yu, P-A. Glaude, Exploring and Modeling the Chemical Effect of a Cetane Booster Additive in a Low-Octane Gasoline Fuel, SAE Technical Paper 2019-24-0069 (2019).
- [14] M. D. Le, M. Matrat, A. Ben Amara, F. Foucher, B. Moreau, Y. Yu, P-A. Glaude, Experimental and Numerical Investigation of the Promoting Effect of a Cetane Booster in a Low-Octane Gasoline Fuel in a Rapid Compression Machine: a Study of 2-Ethylhexyl Nitrate, *Combustion and Flame* 222 (2020) 36–47.
- [15] A.M. Danilov, Fuel additives: Evolution and Use in 1996–2000, *Chemistry and Technology of*

- Fuels and Oils 37 (2001) 444–455.
- [16] P.A. Bonczyk, Effect of Ferrocene on soot in a prevaporized iso-octane/air diffusion flame, *Combustion and Flame* 87 (1991) 233–244.
- [17] T. Hirasawa, C.-J. Sung, Z. Yang, A. Joshi, H. Wang, Effect of ferrocene addition on sooting limits in laminar premixed ethylene–oxygen–argon flames, *Combustion and Flame* 139 (2004) 288–299.
- [18] K.E. Ritrievi, J.P. Longwell, A.F. Sarofim, The effects of ferrocene addition on soot particle inception and growth in premixed ethylene flames, *Combustion and Flame* 70 (1987) 17–31.
- [19] K. Tian, Z.S. Li, S. Staude, B. Li, Z.W. Sun, A. Lantz, M. Aldén, B. Atakan, Influence of ferrocene addition to a laminar premixed propene flame: Laser diagnostics, mass spectrometry and numerical simulations, *Proceedings of the Combustion Institute* 32 (2009) 445–452.
- [20] S. Staude, U. Bergmann, B. Atakan, Experimental and Numerical Investigations of Ferrocene-Doped Propene Flames, *Zeitschrift für Physikalische Chemie* 225 (2011) 1179–1192.
- [21] R.L. Vander Wal, L.J. Hall, Ferrocene as a precursor reagent for metal-catalyzed carbon nanotubes: competing effects, *Combustion and Flame* 130 (2002) 27–36.
- [22] Y. Fenard, H. Song, R. Dauphin, G. Vanhove, An engine-relevant kinetic investigation into the anti-knock effect of organometallics through the example of ferrocene, *Proc. Combust. Inst.* 37 (2019) 547–554.
- [23] A.D. Oleinikov, V.N. Azyazov, A.M. Mebel, Oxidation of cyclopentadienyl radical with molecular oxygen, *Combustion and Flame* 191 (2018) 309–319.
- [24] A.R. Ghildina, A.D. Oleinikov, V.N. Azyazov, A.M. Mebel, Reaction mechanism, rate constants, and product yields for unimolecular and H-assisted decomposition of 2,4-cyclopentadienone and oxidation of cyclopentadienyl with atomic oxygen, *Combustion and Flame* 183 (2017) 181–193.
- [25] T. Nakazawa, Y. Kaji, A density functional theory investigation of the reactions of Fe and FeO₂ with O₂, *Computational Materials Science* 117 (2016) 455–467.
- [26] M. Pochet, V. Dias, B. Moreau, F. Foucher, H. Jeanmart, F. Contino, Experimental and numerical study, under LTC conditions, of ammonia ignition delay with and without hydrogen addition, *Proc. Combust. Inst.* 37 (2019) 621–629.
- [27] M.H.G. Jacobs, P.J. Van Ekeren, C.G. De Kruif, The vapour pressure and enthalpy of sublimation of ferrocene, *The Journal of Chemical Thermodynamics* 15 (1983) 619–623.
- [28] M. Mehl, W.J. Pitz, C.K. Westbrook, H.J. Curran, Kinetic modeling of gasoline surrogate components and mixtures under engine conditions, *Proc. Combust. Inst.* 33 (2011) 193–200.
- [29] J. Herzler, M. Fikri, K. Hitzbleck, R. Starke, C. Schulz, P. Roth, G.T. Kalghatgi, Shock-tube study of the autoignition of n-heptane/toluene/air mixtures at intermediate temperatures and high pressures, *Combustion and Flame* 149 (2007) 25–31.
- [30] M. Hartmann, I. Gushterova, M. Fikri, C. Schulz, R. Schießl, U. Maas, Auto-ignition of toluene-doped n-heptane and iso-octane/air mixtures, *Combustion and Flame* 158 (2011) 172–178.
- [31] K.E. Lewis, G.P. Smith, Bond dissociation energies in ferrocene, *J. Am. Chem. Soc.* 106(1984)

4650–4651.

- [32] W. Tsang, Chemical Kinetic Data Base for Combustion Chemistry Part V. Propene, Journal of Physical and Chemical Reference Data 20 (1991) 221.
- [33] M.S. Stark, Addition of Peroxyl Radicals to Alkenes and the Reaction of Oxygen with Alkyl Radicals, J. Am. Chem. Soc. 122 (2000) 4162–4170.
- [34] M.D. Rumminger, D. Reinelt, V. Babushok, G.T. Linteris, Numerical study of the inhibition of premixed and diffusion flames by iron Pentacarbonyl, Combustion and Flame 116 (1999) 207–219.
- [35] J.M.C. Plane, R.J. Rollason, A study of the reactions of Fe and FeO with NO₂, and the structure and bond energy of FeO₂, Phys. Chem. Chem. Phys. 1 (1999) 1843–1849.
- [36] A. Giesen, J. Herzler, P. Roth, High temperature oxidation of iron atoms by CO₂, Phys. Chem. Chem. Phys. 4 (2002) 3665–3668.
- [37] J.Z. Wen, C.F. Goldsmith, R.W. Ashcraft, W.H. Green, Detailed Kinetic Modeling of Iron Nanoparticle Synthesis from the Decomposition of Fe(CO)₅, J. Phys. Chem. C 111 (2007) 5677–5688.
- [38] Reaction Design, CHEMKIN-PRO, San Diego, 2017.
- [39] S. Tanaka, F. Ayala, J.C. Keck, A reduced chemical kinetic model for HCCI combustion of primary reference fuels in a rapid compression machine, Combustion and Flame 133 (2003) 467–481.

List of Supplementary materials

File name	Contents
Supplementary_document	<p>Table S1. Composition (molar basis) of gas mixtures in RCM experiments</p> <p>Table S2. Kinetic constant of reactions of ferrocene</p> <p>Table S3. Kinetic constant of reactions of new proposed reactions involving $\text{FeC}_{10}\text{H}_{10}$, FeC_5H_5 and $\text{Fe}(\text{OH})_2$.</p> <p>Figure S1. Pressure history of RCM experiments of the neat surrogate fuel and the surrogate fuel doped with 0.1% mol. ferrocene at $P_c = 10$ bar, $T_c = 830$ K, $\phi = 1$. Experiments and simulations data are noted as EXPE and SIMU respectively. Simulations are conducted with both the initial and updated kinetic models.</p>